

Distribution of Exposure Concentrations and Doses for Constituents of Environmental Tobacco Smoke

Judy S. LaKind,¹ Michael E. Ginevan,² Daniel Q. Naiman,³ Anthony C. James,⁴ Roger A. Jenkins,⁵ Michael L. Dourson,⁶ Susan P. Felter,⁶ Carol G. Graves,^{7,8} and Robert G. Tardiff⁷

The ultimate goal of the research reported in this series of three articles is to derive distributions of doses of selected environmental tobacco smoke (ETS)-related chemicals for nonsmoking workers. This analysis uses data from the 16-City Study collected with personal monitors over the course of one workday in workplaces where smoking occurred. In this article, we describe distributions of ETS chemical concentrations and the characteristics of those distributions (e.g., whether the distribution was log normal for a given constituent) for the workplace exposure. Next, we present population parameters relevant for estimating dose distributions and the methods used for estimating those dose distributions. Finally, we derive distributions of doses of selected ETS-related constituents obtained in the workplace for people in smoking work environments. Estimating dose distributions provided information beyond the usual point estimate of dose and showed that the preponderance of individuals exposed to ETS in the workplace were exposed at the low end of the dose distribution curve. The results of this analysis include estimations of hourly maxima and time-weighted average (TWA) doses of nicotine from workplace exposures to ETS (extrapolated from 1 day to 1 week) and doses derived from modeled lung burdens of ultraviolet-absorbing particulate matter (UVP) and solanesol resulting from workplace exposures to ETS (extrapolated from 1 day to 1 year).

KEY WORDS: 16-City Study; distributional analysis; dose distributions; environmental tobacco smoke; Monte Carlo; nicotine; solanesol; ultraviolet-absorbing particulate matter; workplace exposure.

1. INTRODUCTION

The 16-City Study^(1,2) used personal monitors to measure workplace and away-from-work exposure of nonsmokers to three gas-phase and five particulate-

phase constituents of environmental tobacco smoke (ETS). In this series of three articles, we concentrate on study participants from workplaces where smoking occurred: cell 1 (smoking work, smoking home) and cell 3 (smoking work, nonsmoking home). In the first article, we determine that the concentrations measured in this study are representative of current exposure experienced by nonmanufacturing workers in workplaces where smoking is reported. The second article shows that nicotine, although exhibiting complex decay kinetics, is a good marker for other gas-phase constituents of ETS and for ultraviolet-ab-

Cell definitions were based on self-reported smoking status of home and work.

¹ LaKind Associates, LLC.

² M. E. Ginevan and Associates.

³ The Johns Hopkins University, Department of Mathematical Sciences.

⁴ A. C. James and Associates.

⁵ Oak Ridge National Laboratory.

⁶ TERA.

⁷ The Sapphire Group, Inc., 3 Bethesda Metro Center, Suite 700, Bethesda, MD 20814.

⁸ To whom all correspondence should be addressed.

sorbing particulate matter (UVPM), a particulate-phase constituent. We conclude that UVPM and fluorescing particulate matter (FPM) are highly correlated and far superior to respirable suspended particulate matter (RSP) as particulate markers for ETS exposure.

In this article, we investigate the distribution of the exposure data and illustrate the pattern of exposure across the range of observed concentrations. We employ a distributional analysis approach with the 16-City Study data to determine the distribution of doses of selected ETS constituents likely to be encountered by 73 million nonmanufacturing workers in U.S. workplaces.

2. DISTRIBUTIONAL FITS FOR ETS CONSTITUENT CONCENTRATIONS

The first step in attempting to fit distributions for the constituent concentrations in cell 1 (smoking workplace, smoking home) and cell 3 (smoking workplace, nonsmoking home) was to filter out 17 participants from the study.² Sixteen participants whose time at work did not meet or exceed 1 hour were removed from consideration because it was noted that the most likely reason for the short sampling duration was pump failure. One participant with an anomalously high nicotine level (nine times higher than any other nicotine observation), but without correspondingly high levels of other ETS constituents, also was excluded from the database for this analysis.

Chemical constituent data were examined for the remaining 175 participants in cell 1 and 294 participants in cell 3. Negative concentrations were set equal to 0 because actual concentrations must be positive, and 0 is the closest "physically possible" value to the measured value. A representative histogram (before any negative values were set at 0) for the concentration data for nicotine in cell 1 is shown in Fig. 1. The primary observation was that for each of the constituents and for each of the cells under consideration, the distributions were heavily skewed, with a rapidly decaying probability density as the concentration increased from 0. Incorporation of all of the data, including high outliers, led to a scale in which the observations were highly concentrated in

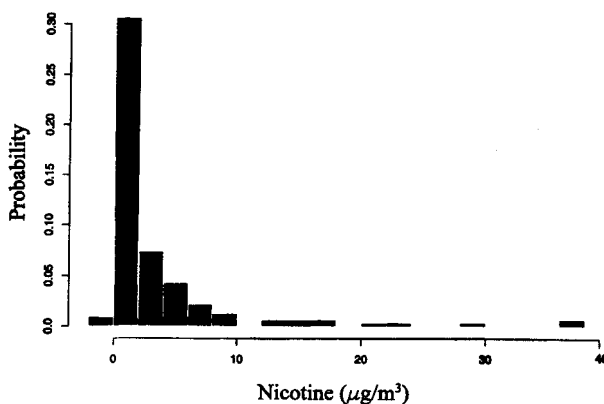


Fig. 1. Histogram showing distribution of workplace nicotine concentrations to which study participants in cell 1 (smoking work, smoking home) were exposed.

small intervals about 0. Hence, the histogram reveals little about the shape of the underlying constituent probability distribution.

Chemical concentrations in studies of this nature tend to be log normally distributed,⁽³⁾ providing an *a priori* reason for testing the hypothesis of log normality for each of the distributions. An additional reason for focusing on this or other parametric family hypotheses is that we sought simple and familiar descriptions of the distributions for ease of interpretation, provided such descriptions exist. We therefore transformed the data by taking base 10 logarithms. Because some of the observed concentrations were 0, and because the logarithm of 0 is not defined, each distribution was fitted in two steps. First, the probability of a 0 value being observed was estimated. The results are given in Table I for all cells and all constituents.

As the results in Table I demonstrate, the probability of a positive workplace concentration for a constituent is smaller for cell 4 (nonsmoking work, nonsmoking home) than for cell 2 (nonsmoking work, smoking home), and the differences in these probabilities can be quite pronounced. For example, the 3-ethenyl pyridine (3-EP) probabilities are .67 and .84, respectively. For myosmine, the probabilities are 0.44 and 0.67. This suggests that the away-from-work environment (smoking vs. nonsmoking) has a decided effect on exposure in nonsmoking workplaces. The same pattern held in the smoking workplace cells (cells 1 and 3) for all of the constituents with the exception of FPM and RSP (i.e., the probability of observing a positive workplace constituent concentration was greater for cell 1 than for cell 3). In the

² Jenkins *et al.*^(1,2) excluded 66 study participants based on average saliva cotinine higher than 15 ng/mL, indicating that these people may have been at least occasional smokers.

Table I. Number of Positive (i.e., Detected) Observations (First Line) for Each Environmental Tobacco Smoke Constituent with the 95th Percentile Confidence Interval for the Probability of a Positive (i.e., Detected) Observation in the Workplace (Second Line)

Constituent	Average detection limits ³	Cell 1 Smoking workplace, smoking home	Cell 2 Nonsmoking workplace, smoking home	Cell 3 Smoking workplace, nonsmoking home	Cell 4 Nonsmoking workplace, nonsmoking home
Nicotine	.027 $\mu\text{g}/\text{m}^3$	172 .98	223 .92	288 .98	718 .86
3-EP	.011 $\mu\text{g}/\text{m}^3$	163 .93	205 .84	271 .92	561 .67
Myosmine	.009 $\mu\text{g}/\text{m}^3$	148 .85	162 .67	239 .81	362 .43
FPM	.272 $\mu\text{g}/\text{m}^3$	173 .99	239 .98	293 1.00	811 .97
UVP	.479 $\mu\text{g}/\text{m}^3$	172 .98	241 .99	289 .98	805 .96
RSP	15.4 $\mu\text{g}/\text{m}^3$	165 .94	226 .93	285 .97	774 .93
Scopoletin	.485 ng/m^3	147 .84	148 .61	224 .76	454 .54
Solanesol	.006 $\mu\text{g}/\text{m}^3$	97 .55	39 .16	130 .44	78 .09
Total number in cell		175	243	294	835

3-EP = 3-ethenyl pyridine, FPM = fluorescing particulate matter, UVP = ultraviolet-absorbing particulate matter, RSP = respirable particulate matter.

smoking workplace cells, the differences in these probabilities tend to be small (less than .04) for all constituents, with the exception of scopoletin (.84 for cell 1 and .76 for cell 3) and solanesol (.55 for cell 1 and .43 for cell 3).

Having calculated the probability of a positive concentration for a given constituent and cell, the next step was to investigate the distribution of \log_{10} constituent concentrations among the positive concentrations. These conditional distributions (conditioned on the data having positive values) are illustrated in Figs. 2 to 9, which show estimates of the probability densities for the eight ETS constituents examined in this study. These figures show the distribution of the log-transformed ETS constituent concentrations obtained in the workplace and use kernel smoothing. Only cells 1 and 3 are considered here, because these are the bases for estimating workplace exposures. Figures 2 to 9 illustrate that for all monitored ETS constituents, the concentrations in cell 1 are greater than those in cell 3.

The Kolmogorov-Smirnov test (Lilliefors option) was applied to test the log-normality hypothesis for each constituent/cell distribution. Table II gives the p values for each of these tests. A p value greater

than .10 is interpreted as evidence that the log-normal hypothesis is a plausible one. If the p value is substantially less than .05, the hypothesis of log normality is rejected. Therefore, for cell 1, the log-normal hypothesis is plausible for all constituents except nicotine and solanesol. For cell 3, the log-normal hypothesis appears to be plausible for nicotine, 3-EP, FPM, UVP, and scopoletin, whereas this hypothesis is clearly rejected for myosmine, RSP, and solanesol.

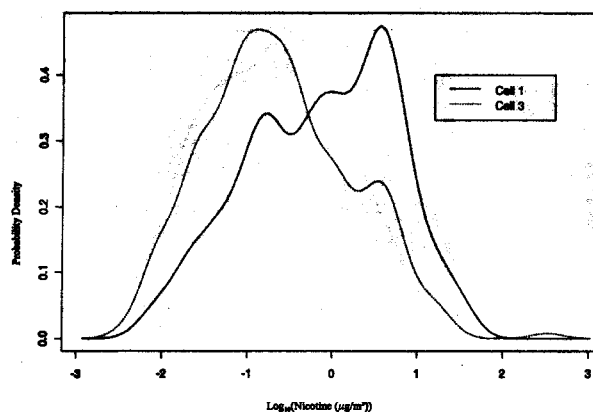


Fig. 2. Conditional distributions (based on detected concentrations) of logarithms of workplace nicotine concentrations for cell 1 (smoking work, smoking home) and cell 3 (smoking work, nonsmoking home) using kernel smoothing.

³ The 24-hour time-weighted-averaged (TWA) limits of detection from Jenkins *et al.* (Table III).⁽²⁾

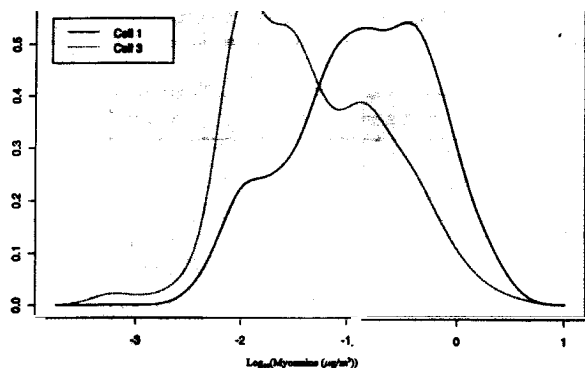


Fig. 3. Conditional distributions (based on detected concentrations) of logarithms of workplace myosmine concentrations for cell 1 (smoking work, smoking home) and cell 3 (smoking work, nonsmoking home) using kernel smoothing.

(Although cells 2 and 4 are not the focus of the investigation, it is observed that the log-normality hypothesis is rejected for all the constituent distributions for these cells.) Describing the underlying distributions when the log-normal hypothesis is accepted is straightforward, because this is reduced to providing estimates of the means and standard deviations of the distributions after the \log_{10} transformations are taken (Table III).

3. APPROACH FOR DISTRIBUTIONAL ANALYSIS OF DOSES

In this research, we used distributional analysis techniques to derive distribution estimates of doses

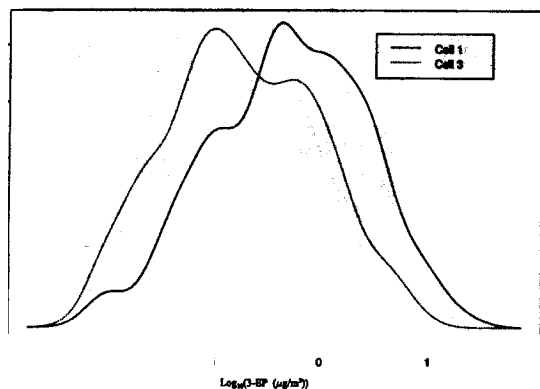


Fig. 4. Conditional distributions (based on detected concentrations) of logarithms of workplace 3-ethyl pyridine (3-EP) concentrations for cell 1 (smoking work, smoking home) and cell 3 (smoking work, nonsmoking home) using kernel smoothing.

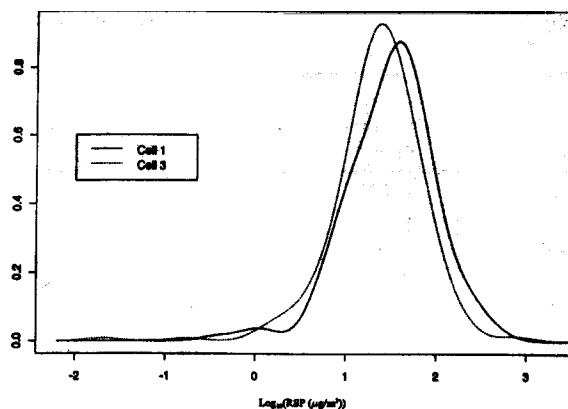


Fig. 5. Conditional distributions (based on detected concentrations) of logarithms of workplace respirable particulate matter (RSP) concentrations for cell 1 (smoking work, smoking home) and cell 3 (smoking work, nonsmoking home) using kernel smoothing.

of ETS-related constituents. Characterization of the chemical concentration distributions in Section 2 guides the subsequent analysis because the distributions are sampled as inputs to the distributional analysis.

There are three basic techniques for representing the chemical data for a distributional analysis.⁽⁴⁾ First, a theoretical or parametric distribution can be fitted to the data using standard statistical techniques. Second, the data can be used to define an empirical distribution function. The third option, called bootstrapping, is to sample the data itself without *a priori* assigning a distribution to the data. Consensus has

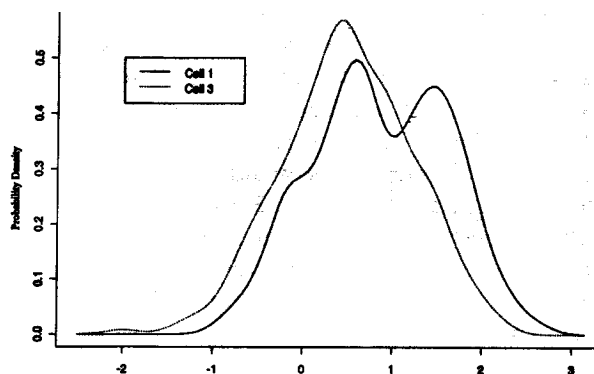


Fig. 6. Conditional distributions (based on detected concentrations) of logarithms of workplace ultraviolet-absorbing particulate matter (UVP) concentrations for cell 1 (smoking work, smoking home) and cell 3 (smoking work, nonsmoking home) using kernel smoothing.

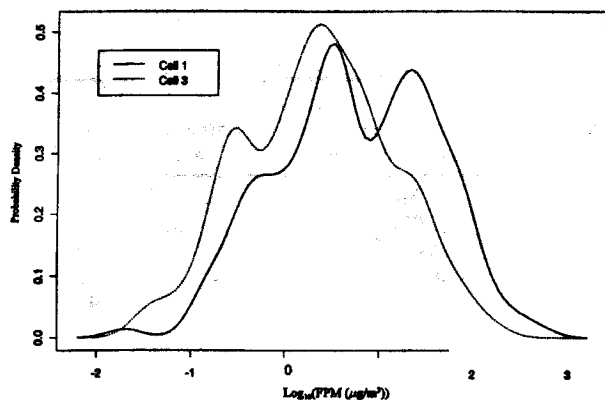


Fig. 7. Conditional distributions (based on detected concentrations) of logarithms of workplace fluorescing particulate matter (FPM) concentrations for cell 1 (smoking work, smoking home) and cell 3 (smoking work, nonsmoking home) using kernel smoothing.

not been achieved on which method is preferable. Generally, selection of the most appropriate technique is left to the discretion of the assessor.⁽⁴⁾

For this study, the results from Section 2 were used as the basis for selection of the appropriate technique. Specifically, for those constituents/cells that could be described by a log normal distribution (e.g., UVPM), a three-parameter approach was used, based on the probabilities defined in Table I (parametric fit) and the statistics presented in Table III. For those constituents/cells that could not readily be described by a log normal distribution (e.g., nicotine and solanesol), the primary data themselves were used as the basis for dose estimations (bootstrap ap-

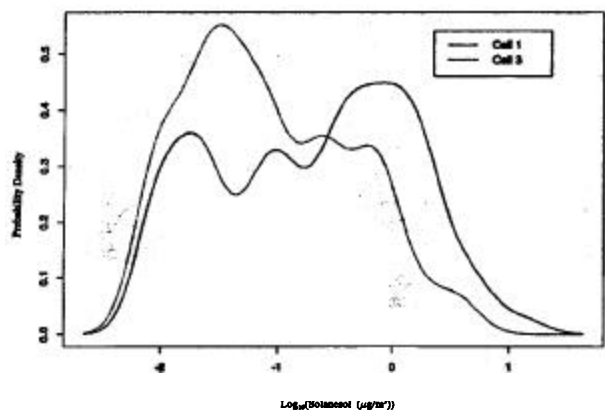


Fig. 8. Conditional distributions (based on detected concentrations) of logarithms of workplace solanesol concentrations for cell 1 (smoking work, smoking home) and cell 3 (smoking work, nonsmoking home) using kernel smoothing.

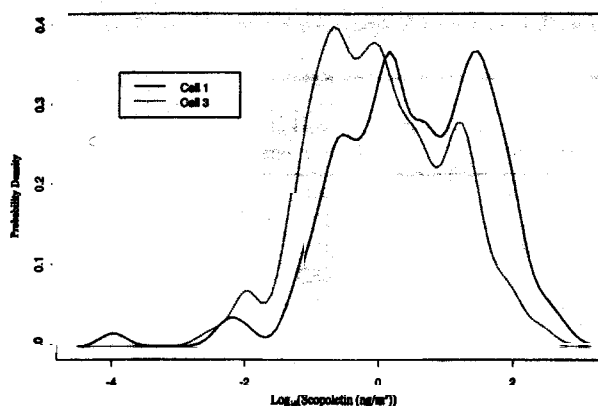


Fig. 9. Conditional distributions (based on detected concentrations) of logarithms of workplace scopolatin concentrations for cell 1 (smoking work, smoking home) and cell 3 (smoking work, nonsmoking home) using kernel smoothing.

proach). For each constituent/cell, the selected approach is listed in Table IV.

4. CHARACTERIZATION OF POPULATION EXPOSURE PARAMETERS

Measured air concentrations of ETS-related chemicals were used to estimate either systemic doses or lung burdens by considering degree of contact. The key parameters in determining dose are exposure duration, body weight, and respiration rate.

Daily exposure durations were derived from data provided by study participants as part of the workplace diary on the number of hours spent sampling ETS-related chemicals at work.^(1,2) These values were considered representative of the general working nonmanufacturing population and used directly in the estimation of gas-phase doses by using the bootstrap method. The distribution for duration of workday was selected by bootstrap sampling from the reported 1,547 work durations (e.g., sampling times, in hours) of the study population. This distribution excluded persons with work durations of 1 hour or less, and one person with an anomalous nicotine exposure. Descriptive statistics for duration of work day are presented in Table V. Perusal of the first quartile (7.44 hours), the median (8.25 hours), and the third quartile (8.29 hours) shows that this is a very tight distribution.

In estimating doses of particulate-phase constituents, it was assumed that, on the average, a workday was 8 hours. This assumption was required due to

Table II. *P*-values for Kolmogorov-Smirnov Test of Log Normality for Positive (i.e., Detected) Environmental Tobacco Smoke Constituent Concentrations

Constituent	Cell 1 Smoking workplace, smoking home	Cell 2 Nonsmoking workplace, smoking home	Cell 3 Smoking workplace, nonsmoking home	Cell 4 Nonsmoking workplace, nonsmoking home
Nicotine	.011	.00010	.082	0
3-EP	>.10	.000030	.085	0
Myosmine	>.10	0	0	0
FPM	.083	0	>.10	.000030
UVPM	.065	0	>.10	.00019
RSP	>.10	.026	0	0
Solanesol	.019	.0020	.00012	0
Scopoletin	.066	.0060	.083	0

3-EP = 3-ethyl pyridine, FPM = fluorescing particulate matter, UVPM = ultraviolet-absorbing particulate matter, RSP = respirable particulate matter.

the inability of the model to incorporate variable exposure durations in estimating particle loading and clearance in the respiratory tract.

For body weight distributions, we used log-normal distributions from Brainard and Burmaster⁽⁵⁾ as given in the Exposure Factors Sourcebook.⁽⁶⁾ For men, the geometric mean and geometric standard deviation are 76.83 and 1.18 kg, respectively, and for women 64.82 and 1.22 kg. It should be noted that there is no unique "best distribution" for human body weight because different populations will have differing distributions. The distributions used here have been widely used, are generally accepted by the

Environmental Protection Agency (EPA),⁽⁷⁾ and are reasonable selections for the purposes of this research.

The probability distribution of breathing rates (minute volumes) for adult indoor workers was developed from the statistical data published by Johnson *et al.*⁽⁸⁾ These data, together with data for other demographic groups from the Cincinnati Activity Diary Study,⁽⁹⁾ were adopted by the EPA in the development of the daily minute volume patterns assumed in the Air Quality Criteria for Particulate Matter document.⁽¹⁰⁾ The full probability distributions of minute volume used in this study were therefore, consis-

Table III. Log₁₀(Constituent) Means (First Line) and Standard Deviations (Second Line) for Positive (i.e., Detected) Environmental Tobacco Smoke Constituent Concentrations

Constituent	Cell 1 Smoking workplace, smoking home	Cell 2 Nonsmoking workplace, smoking home	Cell 3 Smoking workplace, nonsmoking home	Cell 4 Nonsmoking workplace, nonsmoking home
				-1.503
				.650
				-1.320
				.510
				-1.953
				.522
				-.295
				.548
				-.076
				.495
				1.104
				.404
				-.886
				.703
				-1.535
				.628

3-EP = 3-ethenyl pyridine, FPM = fluorescing particulate matter, UVPM = ultraviolet-absorbing particulate matter, RSP = respirable particulate matter.

Table IV. Statistical Method Selected for Each Environmental Tobacco Smoke-Related Constituent for Cells 1 and 3

Constituent	Cell 1	Cell 3
	Smoking workplace, smoking home	Smoking workplace, nonsmoking home
Nicotine	Bootstrap	Bootstrap ⁴
3-EP	Parametric fit	Parametric fit
Myosmine	Parametric fit	Bootstrap
FPM	Parametric fit	Parametric fit
UVPM	Parametric fit	Parametric fit
RSP	Parametric fit	Bootstrap
Solanesol	Bootstrap	Bootstrap
Scopoletin	Parametric fit	Parametric fit

3-EP = 3-ethenyl pyridine, FPM = fluorescing particulate matter, UVPM = ultraviolet-absorbing particulate matter, RSP = respirable particulate matter.

tent with EPA's assumed hourly mean minute volumes for adult indoor workers, as presented in Appendix 10B of that report.⁽¹¹⁾ From the data on respiratory rates, a log-normal breathing rate with a geometric mean of .83 m³/hour (men) or .70 m³/hour (women) was assumed. Geometric standard deviations (GSD) of 1.34 and 1.20 were used for gas- and particulate-phase analyses, respectively.

5. METHODS FOR ESTIMATING DOSES OF ETS-RELATED CHEMICALS

Different methods were used to evaluate gas- and particulate-phase doses, and the available tools for evaluating the two phases differ in terms of complexity, input requirements, and extent of validation. We took care to select tools for which data were available to derive necessary inputs or for which reasonable estimates could be made. We used the distribution described in Section 2 as the basis for estimating systemic dose distributions of the gas-phase nicotine. Because there is insufficient information on the toxicokinetics of myosmine or 3-EP (the other gas-phase constituents measured in the 16-City Study), estimates of systemic doses of these chemicals were not provided. In addition, we modeled estimates of lung burden distributions of UVPM and solanesol, deriving doses from these lung burdens. Lung burdens, rather than systemic doses, for UVPM and solanesol were first estimated because (1) it is not possible to estimate the absorbed dose definitively because

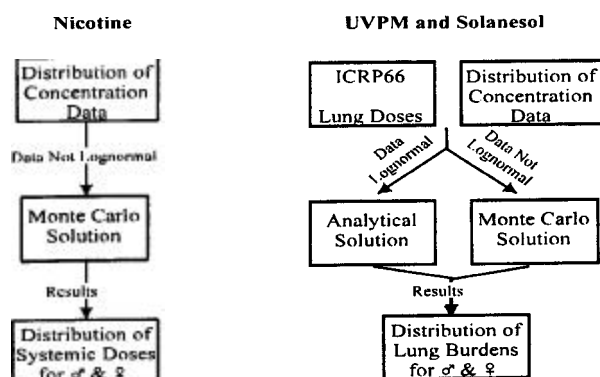
Table V. Descriptive Statistics for Work Duration

N	1547
Mean	8.17
Standard deviation	1.61
Minimum	1.21
First quartile	7.44
Median	8.25
Third quartile	8.92
Maximum	16.97

UVPM is a complex chemical mixture composed of many constituents, each characterized by unique toxicokinetics for which there is little information, and (2) there is insufficient information on solanesol's toxicokinetics to proceed beyond estimates of distributions of doses in the lung.

For the particulate phase, UVPM rather than RSP or FPM was selected for lung burden estimation because (1) the use of RSP as a marker for ETS-RSP has been demonstrated to overestimate exposure to ETS-related compounds⁽¹²⁾ and (2) UVPM and FPM are linearly correlated, with UVPM representing approximately 50% more material than FPM (see second article in this series). Therefore, UVPM provides a more conservative estimate of dose. Because no toxicokinetic/pharmacokinetic information was located on either solanesol or scopoletin, solanesol was selected as an example particulate-phase chemical for modeling lung burden distributions.

In the following sections, we describe the methods used to estimate dose distributions of ETS-related constituents. A summary of the approach used to estimate workplace dose distributions of nicotine (gas phase) and UVPM and solanesol (particulate phase) is shown schematically in Fig. 10.

**Fig. 10.** Flow chart showing steps in the estimation of doses for selected gas- and particulate-phase environmental tobacco smoke (ETS) constituents.

⁴ The results in Table II indicate that for cell 3, either bootstrapping or parametric fit for nicotine would be justified. We selected bootstrapping to keep the method consistent across cells.

5.1. Gas-Phase Nicotine Parameters

To model systemic doses of nicotine, it was necessary to obtain data about nicotine's absorption and elimination behavior in the human body. Nicotine is absorbed rapidly by the small airways and alveoli of the lung, regardless of the pH of the smoke.⁽¹³⁾ Benowitz and Jacob⁽¹³⁾ hypothesized that the rapid absorption of nicotine from cigarette smoke through the lung was "presumably because of the huge surface area of the alveoli and small airways and dissolution of nicotine into fluid of pH in the human physiologic range, which facilitates transfer across cell membranes." According to the report of Russell and Feyereabend,⁽¹⁴⁾ the pulmonary absorption of nicotine is similar to that of intravenous administration (i.e., 100 percent).

Somewhat disparate results have been reported by Molander *et al.*⁽¹⁵⁾ In a study of 14 healthy smokers, the absorption of nicotine was measured after exposure to a nicotine vapor inhaler for 20 minutes every hour for 11 hours. Two different inhalation techniques were used: shallow frequent sucking (buccal mode) and deep inhalations (pulmonary mode). The authors reported that the mean absolute bioavailability of nicotine was 51% (95 percentile confidence interval of 40–65%) for the buccal mode and 56% (95 percentile confidence interval of 47–67%) for the pulmonary mode. Similarly, Iwase *et al.*⁽¹⁶⁾ reported less than complete absorption of nicotine after inhalation from passive, rather than active, smoking. Iwase *et al.*⁽¹⁶⁾ measured the nicotine concentrations in the inspired and expired air of 17 young nonsmoking women exposed passively to tobacco smoking. Based on a total of 47 samples collected from the 17 subjects, absorption was calculated as ranging from 60% to 80% (mean = 71.3%; standard deviation = 10.2%) and was not affected by the nicotine concentration in the inspired air.

In an experiment described by Iwase *et al.*⁽¹⁶⁾ to evaluate the degree of nicotine absorption after nicotine exposure, subjects were asked to inhale cigarette smoke as deeply as possible.⁽¹⁷⁾ The cigarettes were labeled with ¹⁴C, and radioactivity levels were determined in sidestream smoke, cigarette butts, and expired air. Nicotine absorption was calculated, and absorption levels in five smokers were 82%, 84%, 90%, 92%, and 30%, respectively. In three nonsmokers, absorption was determined to be 30%, 53%, and 66%, respectively. Several factors may affect the absorption of nicotine from inhaled smoke and could account for some of the differences in absorption that

have been reported in the literature. These include pH of the smoke,^(13,16) active versus passive smoking,⁽¹⁶⁾ and smoking status.⁽¹⁷⁾

Once absorbed, nicotine is cleared rapidly from the blood as a result of both widespread uptake into tissues and rapid metabolism. Several reports in the literature that cite half-lives for the elimination of nicotine are summarized in Table VI. The terminal half-life of nicotine does not appear to be affected by whether the exposure to nicotine is a single or multiple event⁽²¹⁾. In addition, although the literature provides consistent reports of the half-life for nicotine, significant interindividual differences have been noted^(18,20). Therefore, a terminal half-life for nicotine of about 2 hours appears to be representative of the general human population. Confidence in this value is bolstered by consistent findings in multiple studies that include both smoking and nonsmoking subjects as well as single and multiple exposures.

In summary, nicotine in cigarette smoke is rapidly absorbed in the lungs after inhalation. Studies involving active smoking suggest that the absorption is in the range of 80% to 90%. However, a study on passive smoking in humans measured only 60% to 80% absorption of nicotine. Similarly, a study on absorption of nicotine from a vapor inhaler showed mean values of about 51% to 56%. Once absorbed, nicotine is distributed rapidly throughout the body. The terminal half-life for nicotine in humans is approximately 2 hours, with similar results reported for both smokers and nonsmokers in several independent studies.

The values from this toxicokinetic review that are essential inputs into the characterization of dose distributions are fraction of nicotine absorbed (60–80%) and nicotine half-life in the body (2 hours, but ranging from 1 to 4 hours).

5.2. Gas-Phase Model

The exposure analysis for gas-phase nicotine was conducted as a Monte Carlo simulation, in which each model input was specified as having a particular probability distribution. The distributions for all model inputs are summarized in Table VII. The model equation describing intake (I) of gas-phase components for a fixed time interval T, is

$$I_T = R_h \times T_h \times C_g \times A_g, \quad (1)$$

where

I_T = the intake for an interval of length T in μg

Table VI. Half-Lives for Elimination of Nicotine

Reference	Species	$t_{1/2}$ (min) ⁷	Comments
Robinson <i>et al.</i> ⁽¹⁸⁾	Human	42–360 mean = 112	Half-time used in human PBPK model. Determined from literature.
Benowitz and Jacob ⁽¹³⁾	Human	120	Review article
Zevin <i>et al.</i> ⁽¹⁹⁾	Human (nonsmokers)	103 ± 20.4	IV infusion of 0.5 µg/kg/min over 30 min using radiolabeled nicotine
Benowitz <i>et al.</i> ⁽²⁰⁾	Human (smokers)	119 ± 44	IV infusion in 14 healthy men. Range = ~65 to 150 min, with one outlier with a $t_{1/2}$ of about 240 min.
Feyerabend <i>et al.</i> ⁽²¹⁾	Human (smokers)	133 ± 20	IV infusion of 25 µg/kg nicotine over 1 minute in five subjects, both before and after a loading dose of nicotine from smoking cigarettes (see text below)
Plowchalk <i>et al.</i> ⁽²²⁾	Rat	54 ± 6	After intraarterial injection of 0.1 mg/kg nicotine
Kyerematen <i>et al.</i> ⁽²³⁾	Rat, male	78 ± 6	After IV administration
	Rat, female	108 ± 6	

Rats were exposed to smoke from one cigarette every 8 hours for 15 days (using radiolabeled nicotine the last day).

PBPK = physiologically-based pharmaco-kinetic, IV = intravenous.

R_h = the inhalation rate in m³/hour for the interval

T_h = the length of the interval in hours

C_g = the average concentration of the component during the interval in µg/m³

A_g = the fraction of gas-phase component absorbed into the body (unitless).

The amount of material in the body is also determined by the elimination of the gas-phase constituent

from the body. This process is defined as simple exponential decay:

$$B_t = B_{t-\Delta t} \times e^{-r\Delta t}, \quad (2)$$

where

B_t = the amount of material in the body at time t (body burden in µg)

$B_{t-\Delta t}$ = the amount of material in the body at some past time, $t - \Delta t$

r = the decay constant

Δt = the time interval over which decay takes place.

If Δt is fixed at 1 unit, which will be the “time step” of the final model, $e^{-r\Delta t}$ can be written as a decay constant, D , and Eq. 2 becomes

$$B_t = B_{t-1} \times D \quad (3)$$

Because the value of D is always between 0 and 1, it is clear from the form of Eq. 3 that the amount of material in the body decays by a constant fraction per unit of time. By combining these elements (intake and elimination), the following approximate equation describes the change in body burden over time:

$$B_t = (B_{t-1} \times D) + I \quad (4)$$

The body burden at time t (B_t) is thus defined as the body burden at time $t - 1$ times the decay term D plus the intake during the interval. An exact

Table VII. Summary of Nicotine Model Inputs and Probability Distributions

Input	Units	Distribution
Hourly respiratory rate	m ³ /hour	Log normal with a geometric mean of either .83 (men) or .70 (women). In both cases the GSD is 1.34.
Body weight	kg	Log normal. For men the geometric mean and GSD are 76.83 and 1.18 kg; for women 64.82 and 1.22 kg.
Fraction absorbed	unitless	Uniform between .60 and .80
Half-life in the body	hour	Triangular distribution with most likely value = 2 hours, minimum value = 1 hour, maximum value = 4 hours
Work duration	hour	Bootstrap from 1,547 work durations. Rounded to nearest quarter hour.
Nicotine concentration	µg/m ³	Bootstrap from empirical cell distributions—either 175 values (cell 1) or 294 values (cell 3)

GSD = geometric standard deviation.

⁷ Terminal half-life (i.e., elimination is biphasic, with a rapid initial elimination followed by the terminal phase). The initial $t_{1/2}$ in humans has been reported to be about 9 minutes.⁽²¹⁾

solution, based on integrating the exponential decay function (Eq. 2), with adjustment Z, is given by

$$Z = \frac{1}{E} - \frac{D}{E} = \frac{1-D}{E},$$

where E is equal to minus the natural logarithm of D $[-\ln(D)]$. Any time step can be used to calculate the body burden at any future time equal to a multiple of this time step exactly, assuming continuous exposure within intervals. For example, if the time step is 1 hour, exact body burdens can be calculated at 1, 2, . . . , N hours in the future. Thus, the function of body burden over time can be approximated to any degree of accuracy. The solution to this problem, referred to as the "boundary value problem" in differential equations, is important for dosimetric calculations of time-integrated, or "area under the curve," doses. Thus, the final model equation is

$$B_t = (B_{t-1} \times D) + IZ \quad (6)$$

We have elected to have this model cover only 1 week of exposure. This represents the longest exposure time frame that is relevant because, as a result of nicotine's relatively short physiologic half-life, its presence in the body at the close of work Friday will have been virtually eliminated by the start of the workday on the following Monday. Thus, the dose from one workweek is independent of the previous workweek.

The results of the simulation runs for nicotine are shown in Table VIII, including various percentiles for the hourly maxima (indicated as Max in the table) and time-weighted average exposures (Mean in the table). The model was run 2,000 times for each gender

Table VIII. Nicotine Systemic Doses (in $\mu\text{g/kg}$) for Nonsmokers Exposed to Environmental Tobacco Smoke in the Workplace⁸

Population		Percentiles				
		50th	75th	90th	95th	99th
Men: Cell 1 ⁹	Max ¹¹	.170	.379	.665	.825	1.137
	Mean ¹²	.015	.030	.052	.067	.104
Men: Cell 3 ¹⁰	Max	.065	.131	.298	.447	.658
	Mean	.005	.010	.022	.030	.050
Women: Cell 1	Max	.169	.378	.667	.836	1.143
	Mean	.015	.030	.051	.068	.106
Women: Cell 3	Max	.063	.132	.288	.448	.664
	Mean	.005	.010	.021	.030	.051

⁸ All values are based on 2,000 model simulations.

⁹ Cell 1: Smoking work, smoking home.

¹⁰ Cell 3: Smoking work, nonsmoking home.

¹¹ Max: Maximum hourly body burden.

¹² Mean: Time-weighted average hourly body burden.

(5)

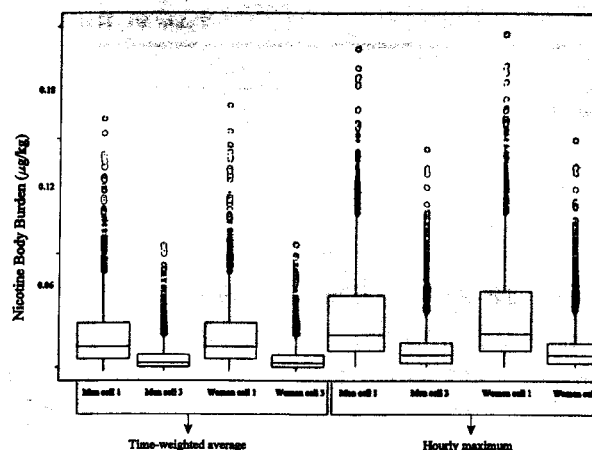


Fig. 11. Time-weighted average and hourly maximum workplace nicotine body burdens for men and women in cell 1 (smoking work, smoking home) and cell 3 (smoking work, nonsmoking home).

in each cell.⁵ The information provided in Table VIII is summarized graphically in box plots in Fig. 11 and in the example histogram in Fig. 12. In general, the nicotine doses for men and women are approximately equal within a cell. Cell 1 participants have higher modeled exposures than cell 3 participants. Both figures illustrate that the distributions are skewed such that most of the study population is at the low end of the dose distribution.

⁵ The Monte Carlo simulation was accomplished using a program written in True BASIC (v. 5.10, 1997).

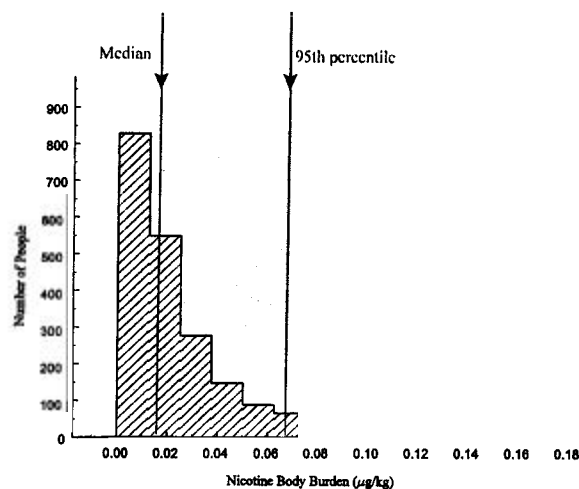


Fig. 12. Distribution of workplace time-weighted average nicotine body burdens for men in cell 1 (smoking work, smoking home) based on 2,000 simulations of the gas-phase dose model.

5.3. Particulate-Phase Model for UVPM and Solanesol

Steady-state lung burdens were estimated for two particulate-phase constituents measured in the 16-City Study. The measured air concentrations of UVPM and solanesol were time-integrated over the course of a workday and used as the basis for extrapolation over the course of a work year. Ideally, time-integrated samples are useful for contaminants whose effects are proportional to a long-term average of the concentration.⁽²⁵⁾ Although this may result in some inaccuracies,⁽²⁶⁾ this extrapolation is reasonable here because, while it is possible that certain individuals experienced unusual exposure during that one-time sampling event, it is unlikely that on the average, the data collected were extreme in either direction. In addition, although workplace exposures to ETS have been declining over the past several years, primarily because of increased restrictions in the workplace, it is reasonable to assume that over the course of 1 year no dramatic decreases will occur. Therefore, it is unlikely that exposures to workplace ETS-related compounds will be significantly overestimated.

Several models have been developed to examine dosimetry of particles in the respiratory tract.^(27,28) For this research, the ICRP Publication 66 Respiratory Tract Model was selected to estimate doses of particulate-phase constituents to regions of the lung. The so-called ICRP66 Lung Model⁽²⁹⁾ incorporates mathematical representations of human data concerning both particle deposition in and clearance from the various functional regions of the respiratory tract.

The practical solution of the ICRP66 model for the adult male is implemented in the software package LUDEP 2.0.⁽³⁰⁾ An earlier version of LUDEP was applied by McAughey *et al.*,⁽³¹⁾ Strong *et al.*,⁽³²⁾ and McAughey⁽³³⁾ to analyze experimental data on the deposition of ETS particulate aerosol in human volunteer subjects. These authors concluded that the ICRP66 Lung Model yielded a reasonable representation of the measured values for experimentally determined aerosol size distributions and participant breathing patterns. Accordingly, the LUDEP 2.0 model implementation was applied here to predict deposited mass and accumulated tissue burdens in the male worker after chronic exposure to ETS particulates in the workplace. The model requires an assumed breathing rate during exposure at work and assumptions concerning ETS aerosol-size distributions and absorption behavior after particle deposition in the respiratory tract. To simulate accumulated

tissue burdens in the female worker, we applied the developmental version of LUDEP (Version 18.1) used to calculate ICRP's reference regional deposition values for adult females and children.⁽²⁹⁾

In this research, we estimated the cumulative mass burden, taking into account reasonable estimates of the absorption characteristics exhibited by various chemical components of the deposited particles. These model assumptions included aerosol mass median diameters (MMD) from .2 μm to .4 μm , $\sigma_g = 1.6$, particle density = 1.0 g/cm^3 , and particle shape factor = 1.0. Also, as proposed by McAughey,⁽³³⁾ for both UVPM and the high-molecular-weight organic material solanesol, we assumed that the absorption behavior was similar to that of a Type M material.⁽²⁹⁾

The estimation of distributions for individual long-term lung burdens of ETS-related particulates relies on assumptions of a steady state, obtained after a long-term exposure to a constant particulate level at a constant breathing rate, with an exposure frequency of 8 hours per day, 5 days per week. Therefore, the estimates of long-term dose are provided with the following caveat: Individual variations in particulate levels, daily breathing rates, and length of the work day were not considered as part of the modeled estimates presented here. This is an artifact of the study design that provided ETS measurement data on single days for a large number of workers, but not for individual workers on multiple days. Thus, the data provide an estimate of variability across workers. Had several measurements for each worker been obtained, one could estimate the variability in exposure for the individual. Instead, we made the conservative assumption that the observed variability was caused by variability with each individual.

The underlying distribution of the UVPM data was log normal (Table II). In cell 1, the geometric mean and geometric standard deviation⁶ were 7.98 and 5.77 $\mu\text{g}/\text{m}^3$. In cell 3 they were 3.25 and 5.26 $\mu\text{g}/\text{m}^3$.

Using the ICRP66 model, we modeled long-term lung burden (LTL) for an exposure period of 50 weeks at 8 hours per day, 5 days per week, to a concentration C , in a particular part of the lung, by the equation

$$\text{LTL} = C k B^n, \quad (7)$$

⁶ The geometric mean and standard deviation were calculated by taking the statistics of the \log_{10} distribution in Table III and expressing them in the untransformed units (i.e., UVPM geometric mean in cell 1 = $10^{0.902} = 7.98 \mu\text{g}/\text{m}^3$).

where k and n are fitted constants, B is the average breathing rate in m^3/hour and C is the average particulate concentration in $\mu\text{g}/\text{m}^3$ in the workplace. Equation 7 expressed on a log scale is

$$\ln(\text{LTL}) = \ln(C) + \ln(k) + n \times \ln(B). \quad (8)$$

The concentration term (C) for UVPM and B are log-normally distributed. Therefore, LTL will have a log-normal distribution with a geometric mean given by the LTL value obtained from Eq. 7 and a geometric standard deviation given by

$$\text{GSD}_{\text{LTL}} = \exp \{[\ln(\text{GSD}_C)^2 + n^2 \times (\ln \text{GSD}_B)^2]^{1/2}\}. \quad (9)$$

This method, referred to as “log-normal error propagation,” is used to derive lung burden distributions for males and females in cells 1 and 3 for UVPM. An additional complication in the model is that the constants k and n are dependent on the aerosol mass median diameter (Table IX).

An alternative modeling paradigm was required for assessing lung burdens of solanesol because, unlike UVPM, solanesol concentration data did not follow a log-normal distribution. The approach to this problem parallels the bootstrap methods used in the gas-phase modeling of nicotine with one complication: 78 of 175 solanesol measurements were 0 (i.e., nondetected) in cell 1, and 164 of 294 solanesol measurements were 0 in cell 3. A further difficulty was that, as for UVPM, the model used to predict lung burdens of particulates (ICRP66) predicts steady-state lung burden as a function of long-term exposure. Whereas it seems unreasonable that long-term exposure would be 0 in a smoking environment, it likewise seems unreasonable to disregard the fact that solanesol exposure is, on the average, 0 (or nondetected) about half the time. Because there is no objective basis for determining the distribution of long-term exposure across individuals, the 0 values were incorporated by multiplying each non-zero value by

the fraction of non-zero observations out of the total number of observations. Thus, for cell 1, each of the 97 non-zero observations was multiplied by 97/175, and for cell 3, each of the 130 non-zero observations was multiplied by 130/294. Furthermore, rather than randomly resampling the solanesol measurements, each value was used a constant number of times to obtain at least 2,000 model simulations. That is, for cell 1 each of the 97 adjusted non-zero solanesol measurements was used 21 times for a total of 2,037 exposure measurements. For cell 3, each of the 130 adjusted non-zero solanesol measurements was used 16 times for a total for 2,080 exposure measurements.

This approach is philosophically and mathematically similar to Latin hypercube sampling, wherein each probability distribution is divided into quantiles (e.g., quintiles, deciles), and an equal number of random measurements is drawn from each quantile. For the model developed here, each measurement was used an equal number of times, which, while not random, was representative. Separate calculations were performed for men and women, for each cell, and for particle mass mean diameters of .2 and .4 μm . For each calculation, a respiratory rate was randomly generated for each exposure measurement. The appropriate coefficients in Eq. 7 (the fitted constants k and n shown in Table IX) were then applied to solve for a lung burden. Because more than 99.9% of total lung burden is alveolar and total dose is the exposure metric of interest, only alveolar lung burdens were estimated.

We emphasize that the LUDEP model results were alveolar burdens in μg . We took these burdens and divided by representative body weights (76.8 kg for men and 64.8 kg for women⁽⁶⁾) to determine doses in $\mu\text{g}/\text{kg}$. Statistical summaries of the UVPM doses derived from the alveolar burden distributions determined via log-normal error propagation by the LUDEP models are given in Table X. Alveolar burdens for men and women, for cells 1 and 3, and for particle mass median diameters of .2 or .4 μm are illustrated in Fig. 13, and Fig. 14 shows an example histogram of UVPM alveolar lung burden in the men in cell 1 for a particle size of .2 μm . Usually, men have higher lung burdens than women in the same cell and for the same particle size. Cell 1 lung burdens are always greater than cell 3 lung burdens, and lung burdens are higher for the smaller particle size. As was the case for nicotine, the UVPM lung burdens are skewed such that most exposed individuals are situated at the low end of the distributions.

Table XI presents percentiles of workplace so-

Table IX. Inputs for the Particulate-Phase Model to Estimate Ultraviolet-Absorbing Particulate Matter and Solanesol Alveolar Burden

	Aerosol mass median diameter = 0.2 μm		Aerosol mass median diameter = 0.4 μm	
	k	n	k	n
Lung tissue				
Alveolar: men	69.5	.849	51.8	.797
Alveolar: women	65.4	1.06	50.1	1.03

Table X. Ultraviolet-Absorbing Particulate Matter Doses (in $\mu\text{g}/\text{kg}$) for Nonsmokers Exposed to Environmental Tobacco Smoke in the Workplace^{8,13}

Population	Percentiles				
	5th	25th	50th	75th	95th
Men: Cell 1, ⁹ MMD ¹⁴ = .2 μm	.312	1.83	6.15	20.7	103
Men: Cell 1, MMD = .4 μm	.246	1.40	4.62	16.4	92.7
Men: Cell 3, ¹⁰ MMD = .2 μm	.148	.808	2.74	8.85	42.1
Men: Cell 3, MMD = .4 μm	.121	.628	2.07	6.56	32.0
Women: Cell 1, MMD = .2 μm	.248	1.61	5.69	20.5	108
Women: Cell 1, MMD = .4 μm	.272	1.46	4.58	15.7	82.8
Women: Cell 3, MMD = .2 μm	.134	.643	2.09	7.11	40.5
Women: Cell 3, MMD = .4 μm	.110	.539	1.81	5.62	32.0

MMD = Aerosol mass median diameter.

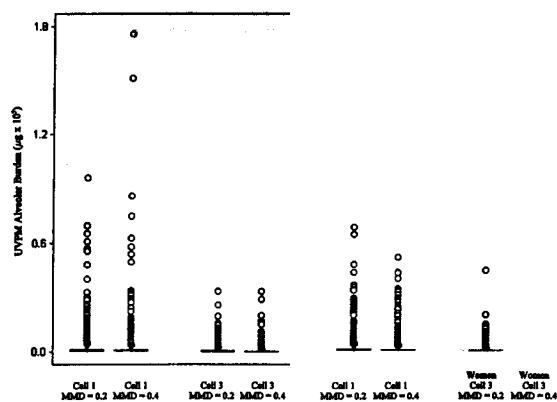
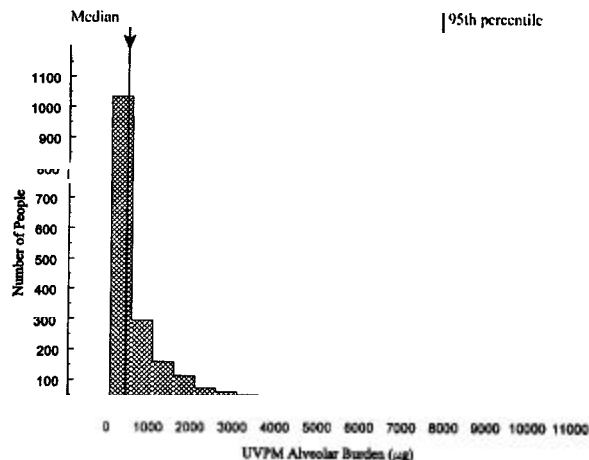
lanesol doses derived from the modeled lung burdens. As for UVP, men have slightly higher doses than women; cell 1 doses are greater than cell 3 doses; and doses are greater for smaller particle sizes. This information is summarized in the box plot in Fig. 15 and the distribution in Fig. 16.

6. DISCUSSION

In this article, we describe (1) distributions of the ETS constituent concentrations collected in cells

¹³ These doses were calculated by dividing the alveolar burden (in μg), estimated using the LUDEP models, by geometric mean body weights (in kg) used with the gas-phase model: 76.8 kg for men and 64.8 kg for women.⁽⁵⁾

¹⁴ MMD: Aerosol mass median diameter.

**Fig. 13.** Workplace ultraviolet-absorbing particulate matter (UVP) alveolar burdens for men and women in cell 1 (smoking work, smoking home) and cell 3 (smoking work, nonsmoking home) exposed to particulate aerosols with mass median diameters (MMD) of .2 or .4 μm .**Fig. 14.** Distribution of workplace ultraviolet-absorbing particulate matter (UVP) alveolar burdens for men in cell 1 (smoking work, smoking home) exposed to particulate aerosols with a mass median diameter (MMD) of .2 μm . Distribution is based on 2,000 simulations of the particulate-phase lung burden model.

1 and 3 of the 16-City Study, (2) characteristics of the study population essential for estimating dose distributions of the ETS-related constituents, (3) the gas- and particulate-phase models for estimating those doses, and (4) the estimated dose distributions of nicotine, UVP, and solanesol for nonsmoking workers from workplace exposure to ETS. We use a distributional approach because of its many advantages over a single-point estimate. This approach is becoming more popular, as evidenced by the increasing number of articles employing it and by its increasing acceptance by regulators. The distributional approach considers the entire population by taking into

Table XI. Solanesol Doses (in $\mu\text{g}/\text{kg}$) for Nonsmokers Exposed to Environmental Tobacco Smoke in the Workplace^{13,15}

Population	Percentiles				
	5th	25th	50th	75th	95th
Men: Cell 1, ⁹ MMD ¹⁴ = .2 μm	.187	.623	4.46	15.6	60.2
Men: Cell 1, MMD = .4 μm	.141	.467	3.40	11.8	45.3
Men: Cell 3, ¹⁰ MMD = .2 μm	.111	.329	.801	3.44	17.5
Men: Cell 3, MMD = .4 μm	.085	.247	.605	2.58	13.1
Women: Cell 1, MMD = .2 μm	.165	.552	3.94	14.7	51.3
Women: Cell 1, MMD = .4 μm	.128	.428	3.07	11.4	40.0
Women: Cell 3, MMD = .2 μm	.096	.297	.718	3.11	16.4
Women: Cell 3, MMD = .4 μm	.075	.230	.558	2.41	12.6

MMD = Aerosol mass median diameter.

¹⁵ Cell 1 values are based on 2,037 model simulations, cell 3 on 2,080 simulations.

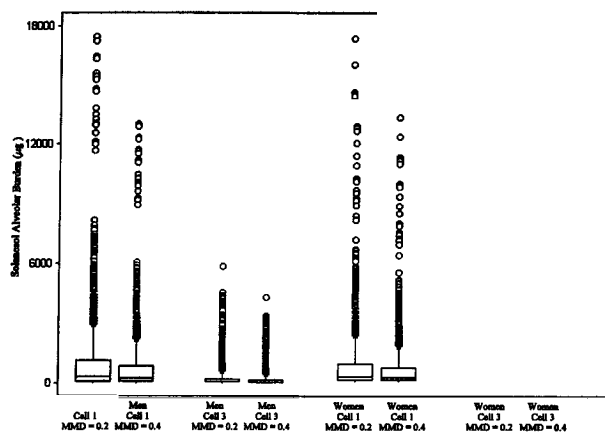


Fig. 15. Workplace solanesol alveolar burdens for men and women in cell 1 (smoking work smoking home) and cell 3 (smoking work, nonsmoking home) exposed to particulate aerosols with a mass median diameter (MMD) of .2 or .4 μm .

account variation in the population. A distribution is more revealing and more scientifically rigorous than a single-point estimate. The distributional approach enables a decision maker to consider the entire distribution of dose (in this case) and tell how much of the population is affected (and consequently what segment of the population might receive benefit by changes in exposure). In this analysis, estimating dose distributions rather than determining point estimates of dose showed that the preponderance of exposed individuals were exposed on the low end of the distribution curve.

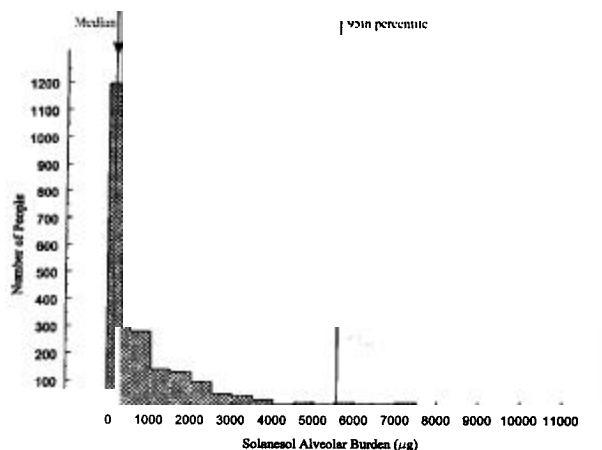


Fig. 16. Distribution of solanesol burdens for men in cell 1 (smoking work, smoking home) exposed to particulate with a mass median diameter (MMD) of .2 μm and based on 2,000 simulations of the particulate-phase lung burden model.

Mean nicotine body burdens (i.e., systemic doses) in men (50th percentile) were estimated to range from .005 to .015 $\mu\text{g}/\text{kg}$, whereas maximum hourly nicotine body burdens in men (99th percentile) were estimated to range from .658 to 1.137 $\mu\text{g}/\text{kg}$. For women, mean nicotine body burdens (50th percentile) were estimated to range from .005 to .015 $\mu\text{g}/\text{kg}$ (same range as for men), whereas maximum hourly nicotine body burdens (99th percentile) were estimated to range from .664 to 1.143 $\mu\text{g}/\text{kg}$ (very slightly higher than the range for men). For both men and women, the distributions were skewed, with doses for most people at the low end of the distribution. In addition, body burdens of nicotine were higher in cell 1 participants (i.e., those also exposed to ETS outside of work) than cell 3 participants (i.e., those from nonsmoking homes).

For men, mean (50th percentile) UVPM doses derived from alveolar burdens (assuming a particle size of .2 μm) were estimated to range from 2.74 to 6.15 $\mu\text{g}/\text{kg}$, whereas the 95th percentile doses were estimated to range from 42.1 to 103 $\mu\text{g}/\text{kg}$. For women, mean UVPM doses derived from alveolar burdens (assuming a particle size of .2 μm) were estimated to range from 2.09 to 5.69 $\mu\text{g}/\text{kg}$, whereas the 95th percentiles were estimated to range from 40.5 to 108 $\mu\text{g}/\text{kg}$. If a particle size of .4 μm were assumed, men's UVPM alveolar burdens and doses were approximately 75% of those assuming the smaller particle size. Women's doses were approximately 80% to 85% of those listed here.

For solanesol, assuming a particle size of .2 μm , 50th percentile dose values in men ranged from .80 to 4.46 $\mu\text{g}/\text{kg}$, whereas 95th percentile doses ranged from 17.5 to 60.2 $\mu\text{g}/\text{kg}$. For women, the 50th and 95th percentile dose values were .72–3.94 $\mu\text{g}/\text{kg}$ and 16.4–51.3 $\mu\text{g}/\text{kg}$, respectively. If the larger particle size was assumed, men's doses were 75% and women's were 78% of the values summarized here. The UVPM and solanesol lung burdens and the resulting doses were skewed such that most people were exposed at the low end of the dose distribution. In addition, men had higher doses than women, and cell 1 doses were greater than cell 3 doses.

The extent to which these results are representative of a broader population is dependent on the representativeness of the study population to the broader population. Generally, the proportion of females participating in the study was greater than in the general U.S. population (first article in the series and Jenkins *et al.*,^(1,2)). In addition, the median income was higher and the representation by white collar

occupations greater in the study population than in the U.S. population. Racial distributions between the study population and the U.S. population were not substantially different. The 16-City Study population had a greater number of people ages 24 to 64 than the general population, most likely because of the requirement that individuals be employed full-time. Due to the nature of the employment requirement, the 16-City Study population more closely reflects the U.S. working, nonmanufacturing population targeted in the Occupational Safety and Health Administration (OSHA) proposed Indoor Air Quality Regulations⁽³⁴⁾ than the general U.S. population. In addition, the ETS workplace data from the 16-City study were not substantially different from those collected by personal monitors in recent workplace studies (first article in this series), suggesting that the dose distributions determined here provide reasonable estimates of ETS exposure in smoking workplaces in the United States.

Approximately 92 million workers are covered by OSHA. This includes postal workers but excludes other public sector employees. About 19 million of these workers are in manufacturing. The doses estimated here from data collected in the 16-City Study are representative of the doses encountered by non-manufacturing workers in workplaces where smoking occurs. An increasing number of workplaces have at least some smoking restrictions. Therefore, the doses estimated here are the upper-bound doses likely to be encountered by approximately 73 million non-manufacturing workers in the United States.

ACKNOWLEDGMENTS

This research was sponsored by the Center for Indoor Air Research, Linthicum, MD. The authors thank P. Price, R. Counts, and M. Morris for their insightful comments on the manuscript.

Data from the 16-City Study used in this series of papers are available on CD-ROM from Carol G. Graves, The Sapphire Group, 3 Bethesda Metro Center, Suite 700, Bethesda, Maryland 20814. Please include a check for \$10 (U.S.) to cover costs.

REFERENCES

1. R. A. Jenkins, M. R. Guerin, A. Palausky, R. W. Counts, C. K. Bayne, and A. B. Dindal, "Determination of Human Exposure to Environmental Tobacco Smoke (ETS): A Study Conducted in 16 U.S. Cities," draft final report by Oak Ridge

- National Laboratory for Center for Indoor Air Research, Linthicum, Maryland (1996a).
2. R. A. Jenkins, A. Palausky, R. W. Counts, C. K. Bayne, A. B. Dindal, and M. R. Guerin, "Exposure to Environmental Tobacco Smoke in Sixteen Cities in the United States as Determined by Personal Breathing Zone Air Sampling," *J. Exposure Anal. Environ. Epidemiol.* 6(4), 473-502 (1996b).
3. W. R. Ott, "A Physical Explanation of the Lognormality of Pollutant Concentrations," *J. Air Waste Manage. Assoc.* 40, 1378-1383 (1990).
4. U.S. EPA (U.S. Environmental Protection Agency), "Guiding Principles for Monte Carlo Analysis," Risk Assessment Forum, Washington, D.C., EPA/630/R-97/001 (March 1997).
5. J. Brainard and D. E. Burmaster, "Bivariate Distributions for Height and Weight of Men and Women in the United States," *Risk Anal.* 12(2), 267-275 (1992).
6. American Industrial Health Council (AIHC), Exposure Factors Sourcebook. Washington, D.C. (1994).
- U.S. Environmental Protection Agency (EPA), "Exposure Factors Handbook," Exposure Assessment Group, Office of Research and Development, Washington, D.C., EPA/600/P-95/002Ba (August 1996a).
8. T. R. Johnson, J. E. Capel, E. Olaguer, and L. Wijnberg, "Estimation of Carbon Monoxide Exposures by Urban Residents Using a Probabilistic Version of NEM," report by IT Air Quality Services for the U.S. Environmental Protection Agency, Office of Air Quality Planning and Standards, Research Triangle Park, North Carolina (1992).
9. T. R. Johnson, "A Study of Human Activity Patterns in Cincinnati, Ohio," report by PEI Associates, Inc., for Electric Power Research Institute, available from Ted R. Johnson, IT Corporation, 3710 University Drive, Durham, NC 27707 (1987).
10. U.S. Environmental Protection Agency (EPA), *Air Quality Criteria for Particulate Matter: Vols. I, II, and III*, Office of Research and Development, Washington, D.C., EPA/600/P-95/001aF (April 1996b).
11. A. C. James, A. M. Jarabek, P. E. Morrow, R. B. Schlesinger, M. B. Snipes, and C. P. Yu, "Dosimetry of Inhaled Particles in the Respiratory Tract," in *Air Quality Criteria for Particulate Matter, Vol. II*, U.S. Environmental Protection Agency, Office of Research and Development, Washington, D.C., EPA/600/P-95/001bF (April 1996).
12. D. J. Eatough, L. D. Hansen, and E. A. Lewis, "Assessing Exposure to Environmental Tobacco Smoke," in R. Perry and P. W. Kirk (eds.), *Indoor and Ambient Air Quality*, pp. 131-140. (Selper Ltd., Chiswick, London, United Kingdom, 1988).
13. N. L. Benowitz and P. Jacob III, "Metabolism, Pharmacokinetics, and Pharmacodynamics of Nicotine in Man," in W. R. Martin, G. R. van Loon, E. T. Iwamoto, and D. L. Davis (eds.), *Advances in Behavioral Biology—Tobacco Smoking and Nicotine: A Neurobiological Approach*, pp. 357-373, (Plenum Press, New York, 1987).
14. M. A. H. Russell and C. Feyerabend, "Cigarette Smoking: A Dependence on High-Nicotine Boli," *Drug Metab. Rev.* 8(1), 29-57 (1978).
15. L. Molander, E. Lunell, S. B. Andersson, and F. Kuylensstierna, "Dose Released and Absolute Bioavailability of Nicotine from a Nicotine Vapor Inhaler," *Clin. Pharmacol. Ther.* 59(4), 394-400 (1996).
16. A. Iwase, M. Aiba, and S. Kira, "Respiratory Nicotine Absorption in Non-smoking Females During Passive Smoking," *Int. Arch. Occup. Environ. Health* 63, 139-143 (1991).
17. A. K. Armitage, C. T. Dollery, C. F. George, T. H. Houseman, P. J. Lewis, and D. M. Turner, "Absorption and Metabolism of Nicotine from Cigarettes," *Br. Med. J.* 4, 313-316 (1975).
18. D. E. Robinson, N. J. Balter, and S. L. Schwartz, "A Physiologically Based Pharmacokinetic Model for Nicotine and Cotinine

- in Man," *J. Pharmacokin. Biopharmaceut.* **20**(6), 591-609 (1992).
19. S. Zevin, P. Jacob III, and N. Benowitz, "Cotinine Effects on Nicotine Metabolism," *Clin. Pharmacol. Ther.* **61**, 649-654 (1997).
 20. N. L. Benowitz, P. Jacob III, R. T. Jones, and J. Rosenberg, "Interindividual Variability in the Metabolism and Cardiovascular Effects of Nicotine in Man," *J. Pharmacol. Exp. Ther.* **221**(2), 368-372 (1982).
 21. C. Feyerabend, R. M. J. Ings, and M. A. H. Russell, "Nicotine Pharmacokinetics and Its Application to Intake from Smoking," *Br. J. Clin. Pharmacol.* **19**, 239-247 (1985).
 22. D. R. Plowchalk, M. E. Andersen, and J. D. deBethizy, "A Physiologically Based Pharmacokinetic Model for Nicotine Disposition in the Sprague-Dawley Rat," *Toxicol. Appl. Pharmacol.* **116**(2), 177-188 (1992).
 - G. A. Kyerematen, G. F. Owens, B. Chattopadhyay, and J. D. deBethizy, "Sexual Dimorphism of Nicotine Metabolism and Distribution in the Rat: Studies *in Vivo* and *in Vitro*," *Drug Metab. Dispos.* **16**(6), 823-828 (1988).
 24. K. S. Rotenberg and J. Adir, "Pharmacokinetics of Nicotine in Rats After Multiple-Cigarette Smoke Exposure," *Toxicol. Appl. Pharmacol.* **69**, 1-11 (1983).
 25. H. D. Goodfellow, S. Eyre, and J. A. S. Wyatt, "Assessing Exposures to Environmental Tobacco Smoke," in *Environmental Tobacco Smoke: Proceeding of International Symposium at McGill University*, pp. 53-67. D. J. Ecobichon and J. M. Wu, editors. (Lexington Books, Lexington, Massachusetts/Toronto, Canada, 1989).
 26. D. J. Ecobichon, L. C. Holcomb, R. A. Jenkins, Y. S. Kim, S. Liao, T. Malmfors, D. Moschandreas, R. Perry, and J. M. Wu, "Panel Discussion on Exposure and Dose," in D. J. Ecobichon and J. M. Wu (eds.), *Environmental Tobacco Smoke: Proceeding of International Symposium at McGill University*, pp. 79-96 (Lexington Books, Lexington, Massachusetts/Toronto, Canada, 1989).
 27. C. P. Yu, L. Zhang, M. H. Becquemin, M. Roy, and A. Bouchikhi, "Algebraic Modeling of Total and Regional Deposition of Inhaled Particles in the Human Lung of Various Ages," *J. Aerosol. Sci.* **23**(1), 73-79 (1992).
 28. L. Koblinger and W. Hofmann, "Monte Carlo Modeling of Aerosol Deposition in Human Lungs. Part I: Simulation of Particle Transport in a Stochastic Lung Structure," *J. Aerosol. Sci.* **21**(5), 661-674 (1990).
 29. International Commission on Radiological Protection (ICRP), "Human Respiratory Tract Model for Radiological Protection. ICRP Publication 66," *Ann. ICRP* **24**(1-4), 1-482 (1994).
 30. N. S. Jarvis, A. Birchall, A. C. James, M. R. Bailey, and M. D. Dorrian, "LUDEP 2.0. Personal Computer Program for Calculating Internal Doses Using the ICRP Publication 66 Respiratory Tract Model," National Radiological Protection Board, Oxon, United Kingdom, NRPB-SR287 (1996).
 31. J. J. McAughey, D. A. Knight, A. Black, and C. J. Dickens, "Environmental Tobacco Smoke Retention in Humans from Measurements of Exhaled Smoke Composition," *Inhal. Toxicol.* **6**(6), 615-631 (1994).
 32. J. C. Strong, A. Black, D. A. Knight, C. J. Dickens, and J. J. McAughey, "The Regional Lung Deposition of Thoron Progeny Attached to the Particulate Phase of Environmental Tobacco Smoke," *Radiat. Prot. Dosim.* **54**(1), 47-56 (1994).
 33. J. J. McAughey, "Regional Lung Deposition and Dose of Ambient Particulate in Humans by Particle Mass and Number," in *Proceedings of the Particles in Health Symposium, Prague, 1997* (Air and Waste Management Association, Washington, D.C., 1997).
 34. U.S. Department of Labor (DOL), Occupation Safety and Health Administration (OSHA), "Proposed Rule Indoor Air Quality," *Fed. Reg.* **59**(65), 15969-16039 (April 5, 1994).